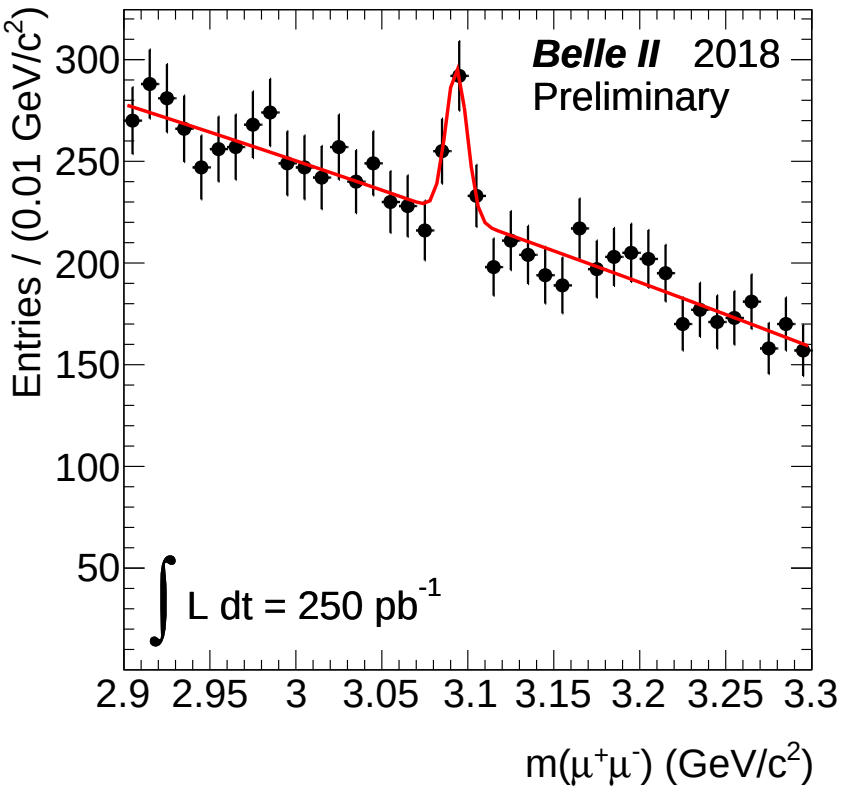

FIG. 1: This figure shows the invariant mass distribution of $J/\Psi \to \mu^+\mu^-$ candidates in 250 pb^{-1} of Phase 2 data. No cuts on the muonID are applied. Selection criteria and further details are described in the internal note BELLE2-NOTE-PH-2018-016.

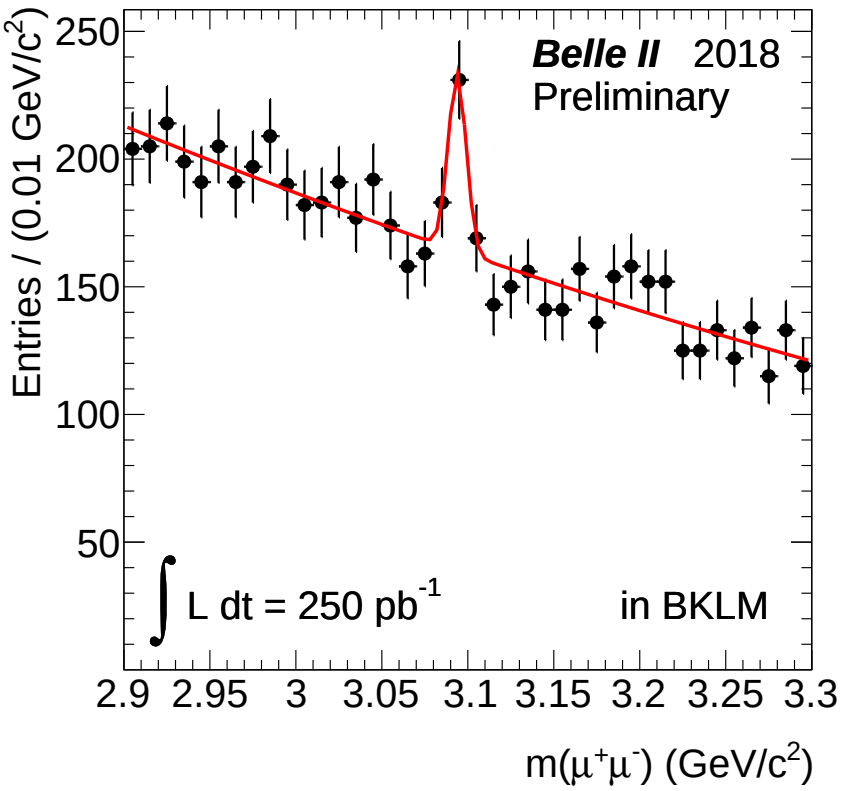

FIG. 2: This figure shows the invariant mass distribution of $J/\Psi \to \mu^+\mu^-$ candidates in 250 pb^{-1} of Phase 2 data. Both tracks are required to point to the BKLM subdetector ($37° < \vartheta_{\mathrm{trk}} < 130°$); no cuts on the muonID are applied. Selection criteria and further details are described in the internal note BELLE2-NOTE-PH-2018-016.

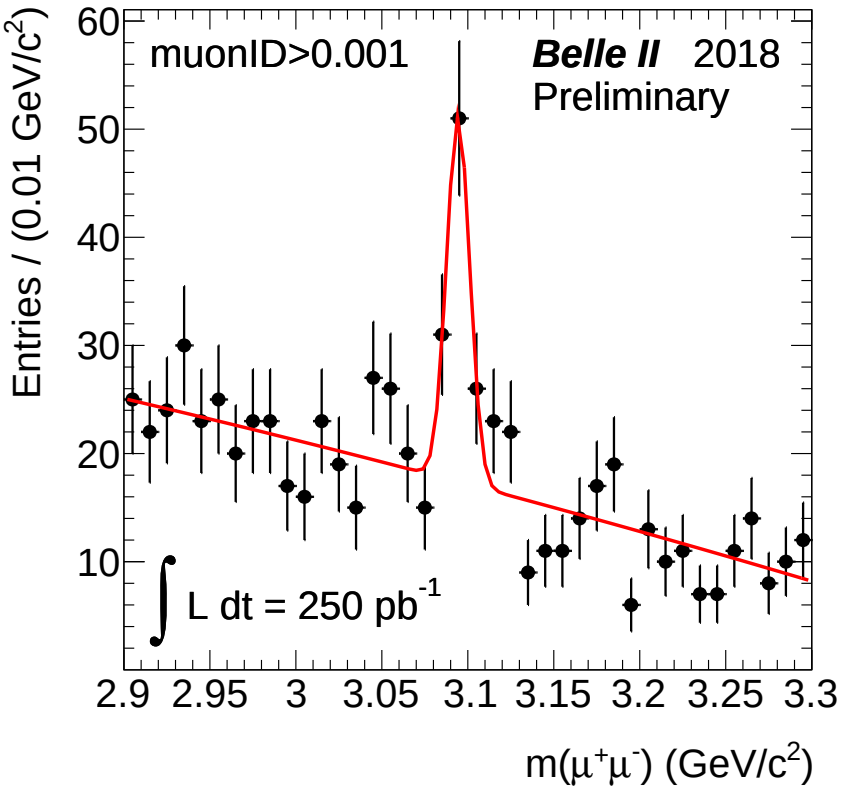

FIG. 3: This figure shows the invariant mass distribution of $J/\Psi \to \mu^+\mu^-$ candidates in 250 pb^{-1} of Phase 2 data. Both tracks are required to point to the BKLM subdetector ($37° < \vartheta_{\text{trk}} < 130°$); at least 1 track is required to have muonID > 0.001 and to have the PID information available from the KLM subdetector. Selection criteria and further details are described in the internal note BELLE2-NOTE-PH-2018-016.